Land Degradation & Development

WILEY

RESEARCH ARTICLE OPEN ACCESS

Simulated Root Exudation Gradient Reveals Dosage-Dependent Carbon Sequestration in Desertification Ecosystems

Ran Xue[1] | Xuemei Fang[1] | Dongming Chen[1] | Fei Yan[1] | Aomei Jia[1] | Zhouwen Ma[1] | Yongheng Gao[2] | Jiqiong Zhou[1] | Jian Zhang[3] | Lin Liu[1]

[1]College of Grassland Science and Technology, Sichuan Agricultural University, Chengdu, Sichuan, China | [2]CAS Key Laboratory of Mountain Ecological Restoration and Bioresource Utilization & Ecological Restoration and Biodiversity Conservation Key Laboratory of Sichuan Province, Chengdu Institute of Biology, Chinese Academy of Sciences, Chengdu, Sichuan, China | [3]Sichuan Development Research Centre of Forestry and Grassland, Chengdu, Sichuan, China

Correspondence: Lin Liu (liulinsky@126.com)

Received: 23 March 2026 | **Revised:** 29 May 2026 | **Accepted:** 1 July 2026

Keywords: ^{13}C-labeling | carbon sequestration | desertification | organic input | priming effect | *Salix cupularis*

ABSTRACT

Root exudates serve as a key driver for the restoration of soil organic carbon (SOC), particularly in aeolian desertification ecosystems where aboveground litter retention is limited. While *Salix cupularis* is widely planted as an effective pioneer shrub for ecological rehabilitation on the Qinghai-Tibet Plateau, how the quantity of its root exudates regulates the dynamics of microbial-derived SOC in sandy soils remains unclear. Using ^{13}C isotope labeling and DNA-SIP, we simulated the root carbon exudation of *S. cupularis* with a glucose gradient: ambient rate (V), half the ambient rate (1/2 V), and twice the ambient rate (2 V) to investigate carbon decomposition pathways in sandy soil. We found that different glucose input levels significantly altered soil carbon components and enriched distinct microbial communities. Under V treatment, a higher proportion of glucose was efficiently incorporated into particulate organic carbon (POC). Conversely, both the 1/2 V and 2 V treatments diverted more glucose toward microbial respiration. While 1/2 V treatment increased microbial biomass, it simultaneously induced a positive priming effect, thereby exacerbating native soil carbon loss. Meanwhile, 2 V treatment significantly reduced microbial diversity and further elevated respiration, resulting in the lowest carbon sequestration efficiency. This study elucidates the mechanisms underlying microbial adaptation to varying nutrient inputs and reveals the dosage-dependent advantage of *S. cupularis* root exudation in maintaining soil carbon balance. These findings offer novel perspectives on optimizing carbon sequestration strategies and understanding the ecological restoration capacity of pioneer plants in desertified ecosystems.

1 | Introduction

The Tibetan Plateau plays a critical role in global and regional ecological security, underpinned by its unique biodiversity, vast water resources, and significant carbon storage capacity (Huang et al. 2023; Li et al. 2022). These functions are essential for supporting regional economic development and regulating global atmospheric circulation and precipitation patterns. However, since the 1980s, desertification in this region has been expanding in both scale and intensity, driven primarily by climate

Ran Xue and Xuemei Fang contributed equally to this work.

This is an open access article under the terms of the Creative Commons Attribution License, which permits use, distribution and reproduction in any medium, provided the original work is properly cited.

© 2026 The Author(s). *Land Degradation & Development* published by John Wiley & Sons Ltd.

change and anthropogenic activities (Li et al. 2016). Although extensive ecological restoration efforts have curbed this trend, the region's sandy soils, characterized by low soil organic carbon (SOC) stocks and high nutrient leaching, present persistent governance challenges (Ding et al. 2017).

Vegetation restoration is one of the most effective approaches for rebuilding SOC in degraded ecosystems. Vegetation recovery during grassland restoration significantly enhances SOC accumulation, yielding overall increases ranging from 9% to 42% (Ascenzi et al. 2025). Furthermore, the composition of SOC also shifts from microbe-derived MAOC to plant-derived POC during restoration (Liao et al. 2023). In sandy aeolian ecosystems, however, wind erosion readily removes aboveground litter, making belowground carbon inputs particularly important. Root exudates therefore represent a major pathway through which plants deliver photosynthetically fixed carbon into soil and regulate plant-microbe-soil carbon dynamics.

Root exudates can affect soil organic matter (SOM) through several pathways. As readily available substrates, exudates can support microbial growth, increase microbial biomass, and promote microbial residue formation, thereby contributing to SOM accumulation through the microbial carbon pump (Liang et al. 2024). Root exudates can also modify the rhizosphere environment by changing pH, nutrient availability, mineral-organic interactions, and microbial community composition (Chari and Taylor 2022; Yan et al. 2025). However, their effects on SOC are not always positive. Labile exudates may stimulate microbial respiration and extracellular enzyme production, thereby accelerating the decomposition of native SOM through a positive priming effect (Yuan et al. 2018). Therefore, root exudates may either promote SOM formation or enhance SOM decomposition, depending on how exudate-derived carbon is used by soil microorganisms.

The direction and magnitude of root exudate effects depend on both exudate quality and quantity. Root exudates primarily consist of sugars, amino acids, organic acids, fatty acids, and phenolic compounds (Badri and Vivanco 2009; Yuan et al. 2018). These compounds can have contrasting effects on soil carbon cycling. For instance, sugars and amino acids are readily used by microorganisms and may promote microbial biomass and necromass formation, whereas organic acids may desorb MAOC or increase the accessibility of protected SOM, thereby stimulating decomposition (Yu et al. 2024). In contrast, exudate quantity determines how much labile carbon enters the soil and whether microbial communities allocate this carbon mainly to growth, respiration, or SOM decomposition. When labile carbon inputs are too low, however, microorganisms may continue to decompose native SOM to acquire energy or nutrients (Kuzyakov et al. 2000). When inputs are excessive, microbial anabolic demand may become saturated, and a larger proportion of carbon may be lost as CO_2 through respiration. Thus, the same exudate compound may promote carbon retention at one input level but carbon loss at another.

Despite increasing recognition that both quality and quantity matter, these two factors often vary simultaneously in natural root systems (Luo et al. 2016). Root exudation changes with plant phenology, diurnal rhythm, nutrient status, drought, temperature, and other environmental stressors, making it difficult to determine whether changes in SOC dynamics are driven by exudate composition, exudate amount, or their interaction (Lange et al. 2015; Robert et al. 2025). Glucose is one of the most abundant monomeric sugars in root exudates and is widely used as a chemically defined model substrate to investigate the quantity effect of labile carbon input while minimizing variation in exudate quality (Tao et al. 2023). By fixing exudate quality and manipulating glucose addition rate, it is possible to test whether different degrees of carbon input change microbial respiration, priming, microbial assimilation, and the allocation of exudate-derived carbon among CO_2, microbial biomass, POC, and MAOC.

In the ecological restoration of desertified alpine meadows in the eastern Tibetan Plateau, the native shrub *Salix cupularis* has been widely used as a pioneer species because of its strong adaptability and important role in sand stabilization, wind erosion control, water conservation, nutrient retention, and understory vegetation recovery (Li et al. 2025). Previous studies have shown that *S. cupularis* can form a "resource island" effect, improve soil moisture and nutrient availability, and increase SOC during restoration (Hu et al. 2018; Li et al. 2021). Our previous work further suggested that root-derived compounds from *S. cupularis* can enhance microbial biomass and promote nitrogen fixation by regulating rhizosphere conditions (Yan et al. 2025). These studies demonstrate the positive role of *S. cupularis* in sandy soil restoration, but they do not explain whether the amount of root-derived carbon input itself is a key reason for its capacity to promote SOC accumulation. This leaves an important knowledge gap: although root exudates are recognized as a major pathway of carbon input during *S. cupularis* restoration, the quantity effect of this input on SOC decomposition and formation in sandy soil remains unclear. In particular, it is unknown whether the natural root exudation rate of *S. cupularis* represents an effective carbon input level for microbial-mediated SOC sequestration, or whether lower or higher input levels would shift carbon fate toward priming, respiration, or different SOC fractions.

To address this knowledge gap, we collected sandy soil from a desertified grassland on the Tibetan Plateau and conducted a controlled laboratory incubation experiment using ^{13}C isotope labeling coupled with DNA stable isotope probing (DNA-SIP). Critically, the glucose concentration was manipulated across three levels anchored to the empirically measured natural root exudation rate of *S. cupularis*: half the ambient rate ($1/2\,V = 40\,\mu g$ C day^{-1}), the ambient rate ($V = 80\,\mu g$ C day^{-1}), and twice the ambient rate ($2\,V = 160\,\mu g$ C day^{-1}). We hypothesized that (1) glucose-derived carbon would show a nonlinear response to input quantity. (2) Different glucose input levels would activate distinct microbial communities, thereby regulating the partitioning of exudate-derived carbon among CO_2, microbial biomass, POC, and MAOC. These hypotheses are grounded in the microbial carbon pump framework. Specifically, they build on the premise that the quantity and stoichiometry of available carbon shape microbial strategies, which ultimately govern community-level carbon use efficiency and the fate of plant-derived carbon in soil (Liang et al. 2024).

2 | Material and Methods

2.1 | Study Area

The study site is located within the "National Demonstration Area of Desertification Grassland Restoration" in Zoige County (N 33°43′, E 102°27′, elevation 3430 m a.s.l.; Figure S1). This region experiences a highland cold-temperate humid monsoon climate, characterized by an annual precipitation of 648.5 mm and average annual temperature of 1.1°C. The soil is classified as a typical aeolian sand type (FAO Classification System, 1974) with loose structure and poor erosion resistance. The topography features undulating plateaus with extensive mobile and semi-mobile dunes in desertified areas, interspersed with interdune depressions. Since 1993, native plants, particularly the well-adapted shrub *S. cupularis*, has been planted individually in the desertified alpine grassland. Grid-like sand barriers have been established to facilitate vegetation development. To facilitate vegetation establishment, grid sand barriers were constructed, protective fencing was erected, and dedicated personnel were assigned for minimal-interference management. Through continuous replanting and natural regeneration, a thriving *S. cupularis* population has been established, with an understory community dominated by *Equisetum ramosissimum*, *Carex praeclara*, *Elymus sibiricus*, and *Astragalus zacharensis*. The soil chemical properties at the sampling site were as follows: pH 7.85; bulk density 1.48 g cm^2; soil water content 3.12 (%); organic carbon, 3.20 mg g^{-1}; total nitrogen, 0.10 mg g^{-1}; NO_3^--N, 1.63 mg g^{-1}; NH_4^+-N, 0.53 mg g^{-1}.

2.2 | Experimental Design

In June 2023, five sampling points spaced more than 1 km apart were randomly selected within the field site. At each point, three soil cores (0–15 cm) were collected using a soil corer. The samples were transported to the laboratory, homogenized, air-dried, and passed through a 2 mm sieve, yielding a total of 20 kg of prepared soil for the incubation experiment. The experiment comprised four treatments with four replicates each: a control (CK) receiving deionized water only, and three levels of ^{13}C-glucose addition. The glucose addition rates were based on the in situ root exudation rate of *S. cupularis* measured in our previous work, corresponding to half (1/2 V = 40 μg C day^{-1}), equal to (V = 80 μg C day^{-1}), and double (2 V = 160 μg C day^{-1}) of the natural exudation rate (per root surface area, cm^{-2}).

The incubation experiment was conducted in custom-made, dark, sealed microcosms (cylinders with a diameter of 7 cm and height of 40 cm; Figure S1). Each microcosm was filled with 1 kg of air-dried soil. To simulate continuous root exudation, eight artificial roots (soil solution samplers, Rhizosphere Research Products, Netherlands) with a pore size of 0.12–0.18 μm were uniformly embedded in the soil. For the first 5 days, all microcosms received an equal amount of deionized water to stabilize the system and restore in situ soil moisture. Beginning on Day 6, treatment solutions were continuously injected into the artificial roots for 30 days. The daily glucose-C additions per microcosm were 6.28 mg (1/2 V), 12.56 mg (V), and 25.12 mg (2 V), respectively, applied in 2 mL of solution per day.

2.3 | Sample Analysis

Throughout the 35-day incubation, CO_2 efflux was trapped in 0.5 M NaOH solutions, which were replaced and analyzed for concentration and isotopic ratio ($\delta^{13}C$) at 6-day intervals. The contributions of initial SOM and glucose to the total CO_2 (C_SOM and C_Glu, respectively) were partitioned using isotope mass balance equations (Wang et al. 2019):

$$C_{SOM} = C_{Total} \times \left(C_{Total} - C_{SIP}\right) / \left(C_{Total} - C_{Soil}\right)$$

$$C_{Glu} = C_{Total} \times \left(C_{SIP} - C_{Soil}\right) / \left(C_{Total} - C_{Soil}\right)$$

where C_{Total} is the total amount of CO_2 at the time interval and C_{SIP} is the corresponding isotopic composition, C_{Soil} is the amount of CO_2 derived from the endogenous SOC in the control treatment.

On the final day (Day 35), soil was destructively sampled. From each microcosm, a 100 g subsample was stored at 4°C for microbial biomass carbon (MBC) analysis, and a 200 g subsample was stored at −80°C for DNA extraction and subsequent DNA-based stable isotope probing (DNA-SIP). A final 500-g subsample was air-dried for the analysis of soil carbon fractions: total SOC, particulate organic carbon (POC), and mineral-associated organic carbon (MAOC). The ^{13}C enrichment in all soil carbon pools and CO_2 was measured using an isotope ratio mass spectrometer (Delta Plus XP; Thermo Finnigan MAT).

2.4 | DNA Extraction and DNA Stable Isotope Probing

Total genomic DNA was extracted from 0.5 g of soil using a FastDNA SPIN Kit for Soil (MP Biomedicals, Cleveland, OH, USA) following the manufacturer's protocal. DNA purity and quantity were assessed with a Nanodrop OneC UV–Vis Spectrophotometer (Thermo Fisher Scientific, Waltham, MA, USA). DNA-SIP fractionation was performed as described by Xia et al. (2011). Generally, 2.0 μg DNA was mixed with a CsCl solution to achieve an initial buoyant density of 1.725 g mL^{-1}. The mixture was then subjected to ultracentrifuge at 177,000 g for 44 h at 20°C in a VTi65.2 vertical rotor (Beckman Coulter, Palo Alto, CA, USA). Following centrifugation, the gradient was fractionated from bottom to top by displacement with sterile water using an NE-1000 single syringe pump (New Era Pump Systems Inc., Farmingdale, NY, USA). Fifteen DNA fractions (approximately 380 μL each) were generated and the refractive index of each fraction was determined using an AR200 digital hand-held refractometer (Reichert, Buffalo, NY, USA). DNA from each fraction was precipitated, washed, and resuspended in TE buffer. The V4 region of the bacterial 16S rRNA gene was amplified using primers 515F (5′-GTGCCAGCMGCCGCGGTAA-3′) and 806R (5′-GGACTACHVGGGTWTCTAAT-3′) (Biddle

et al. 2008). Amplicon library was sequenced on an Illumina Hiseq2500 platform (Illumina, San Diego, CA, USA) and paired-end reads of length 250 bp were generated. Raw sequences were then merged, trimmed and filtered. Qualified sequences were clustered into operational taxonomic units (ZOTUs) with USEARCH11. We followed a UNOISE3 pipeline and obtained a total of 9813 ZOTUs across all samples after quality and singleton control (Edgar et al. 2011). Taxonomy was assigned against SILVA RDP training set v16 (Yilmaz et al. 2014) with a confidence cut-off of 80% (Edgar 2016). Relative abundances of the top 10 phyla were selected to give an overview of bacterial composition (Figure S2a).

2.5 | Data Analysis

All the data analyses were performed in R (v4.0.1; https://www.r-project.org/). The OTU table was first rarefied to the same sequencing depth using "phyloseq" package (McMurdie and Holmes 2013). Alpha diversity was assessed with the Shannon index and OTU richness using "vegan" package (Oksanen et al. 2013). Beta diversity was examined via principal co-ordinates analysis (PCoA) based on Bray Curtis dissimilarity matrix with statistical significance tested by PERMONOVA tests (999 permutations). Differentially abundant bacterial taxa across glucose treatments were identified with Linear discriminant analysis Effect Size (LEfSe) using the Kruskal–Wallis rank sum test (Segata et al. 2011). ^{13}C-enriched OTUs in "heavy" SIP fractions were determined using the negative binomial distribution algorithm (DESeq) in "DESeq2" package and visualize with volcano plots (Love et al. 2014). For soil properties and bacterial indices, homogeneity of variances was first tested using Levene's tests. One-way ANOVA followed by Fisher's Least Significant Difference (LSD) post hoc test was applied for comparisons among treatments when variances were homogeneous. Microbial niche width was calculated using the Levins' index implemented in the "spaa" R package (Zhang and Zhang 2013). The correlations between bacterial diversity (Shannon index) and activity (CO_2 flux) with soil pH and C components were analyzed using "ggcor" package (https://github.com/houyunHuang/ggcor).

3 | Results

3.1 | Effect of Glucose Addition on CO_2 Flux

Soil CO_2 release rate increased after glucose/water input and then gradually stabilized. As expected, soil cumulative CO_2 emissions were highest in 2V and lowest in CK, directly reflecting the levels of glucose input (Figure 1a). Due to the priming effect, cumulative CO_2 emission was higher in 1/2V than V. Aligned with the quantity of ^{13}C-glucose added, the cumulative ^{13}C-CO_2 emission was highest in 2V and lowest in 1/2V. For 1/2V, both CO_2 and ^{13}C-CO_2 release rates reached highest on day 30, indicating that microbial activity reached its maximum (Figure 1b). Further, we found a small proportion of ^{13}C-glucose was transformed to ^{13}C-CO_2 in V compared to 1/2V and 2V. This suggested a higher external C sequestration rate under this specific input level.

3.2 | Effect of Glucose Addition on Soil pH and C Components

Our results showed that soil pH was significantly higher in V than other treatments. Most carbon parameters, including SOC, DOC, MAOC, and MBC, reached their highest levels in 2V due to the largest glucose input (Table 1). However, we detected a significantly higher POC in V treatments than CK and 1/2V. Conversely, MBC, DOC, and MAOC in V had no significant differences compared with 1/2V and CK. These results suggested that the added glucose was primarily converted into POC or a lower utilization efficiency of initial POC in V treatments. SOC was lower in 1/2V than in CK after 30 days' incubation, indicating a positive priming effect (Figure S3).

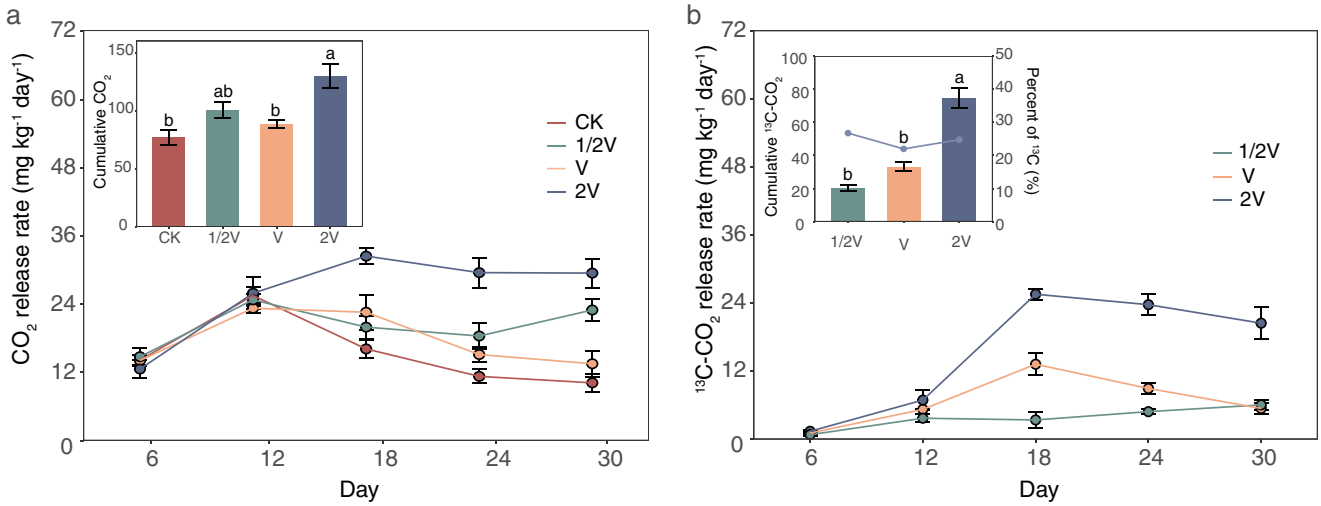


FIGURE 1 | CO_2 release rate, cumulative CO_2 and ^{13}C conversion rate within 30 days' incubation in the three glucose inputs rate (1/2V, V, and 2V root exudation rate of *Salix cupularis*). (a) CO_2 release rate every 6 days. (b) ^{13}C-CO_2 release rate every 6 days. The barplots in the upper left showing cumulative CO_2/^{13}C-CO_2, and the line showing the ^{13}C conversion rate. The error bars showed standard error (SE). [Colour figure can be viewed at wileyonlinelibrary.com]

3.3 | ^{13}C-Glucose Metabolism in Soil

The amount of ^{13}C-SOC was highest in 2V and lowest in 1/2V, while a higher proportion of the added ^{13}C (about 15%) incorporated into ^{13}C-SOC in V compared to other treatments (Figure 2a). No significant differences in ^{13}C-MBC were observed among the treatments, whereas the conversion rate of added ^{13}C to ^{13}C-MBC decreased as the ^{13}C input increased (Figure 2b). Furthermore, ^{13}C-POC and ^{13}C-MAOC were significantly lower in 1/2V compared to other treatments, while the conversion rate of ^{13}C to ^{13}C-POC was higher in V. These results indicated the content of ^{13}C in various carbon components and the corresponding conversion rates within each treatment do not follow a unified linear trend.

3.4 | ^{13}C-Glucose Assimilation by Microbial Communities

Analysis of the ^{13}C-labeled microbial communities revealed a high relative abundance of Acidobacteria (Figure S2a). Volcano plots further demonstrated that ^{13}C-labeled *Candidatus Saccharibacteria* became increasingly prominent with higher glucose inputs (Figure 3a–c). A significant decrease in

TABLE 1 | Soil properties of the three glucose inputs rate (1/2V, V, and 2V root exudation rate of *Salix cupularis*) after 30 days' incubation.

	pH	SOC	MBC	DOC	POC	MAOC
CK	7.27 ± 0.01b	5.36 ± 0.18ab	9.2 ± 0.46b	11.84 ± 0.48b	1.93 ± 0.06bc	0.35 ± 0.03b
1/2V	7.11 ± 0.04b	4.45 ± 0.29b	17.94 ± 1.04b	11.24 ± 1.37b	1.79 ± 0.06c	0.44 ± 0.06ab
V	7.5 ± 0.07a	6.19 ± 0.37a	19.12 ± 3.98b	12.86 ± 1.69b	2.94 ± 0.16a	0.4 ± 0.03b
2V	7.2 ± 0.02b	6.67 ± 0.41a	48.94 ± 5.92a	20.55 ± 1.67a	2.43 ± 0.15ab	0.64 ± 0.07a

Note: Different letters indicate significant differences (one-way ANOVA, LSD test, $p < 0.05$).

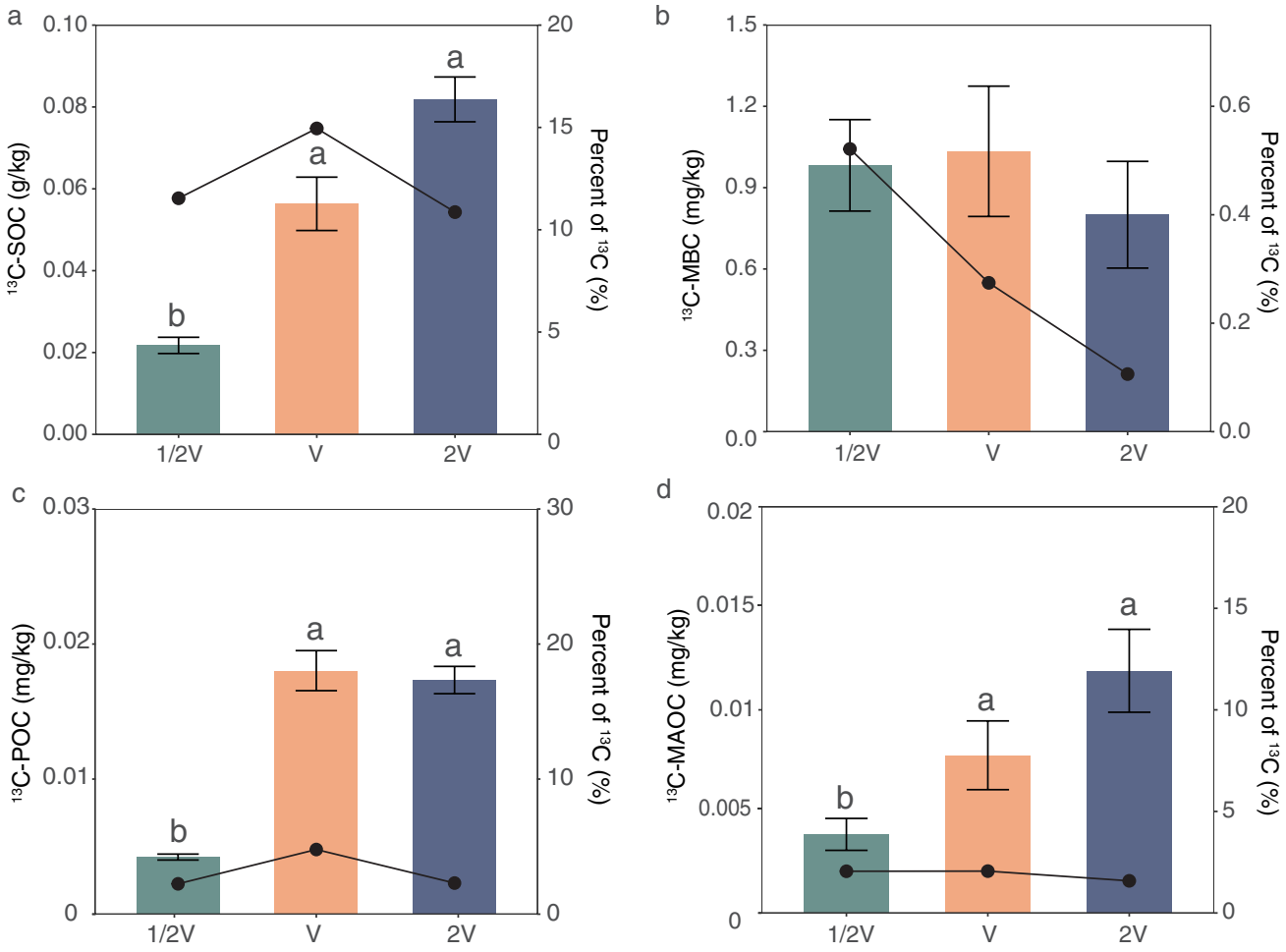


FIGURE 2 | ^{13}C-labeled soil carbon pools ((a) SOC; (b) MBC; (c) POC; (d) MAOC) in the three glucose input rates (1/2V, V, and 2V root exudation rate of *Salix cupularis*) after 30 days' incubation. The line in each barplot shows the ^{13}C conversion rate. The error bars show standard error (SE). [Colour figure can be viewed at wileyonlinelibrary.com]

microbial richness, Shannon index and niche width was observed in 2V treatments (Figures 3d,e and S4). Additionally, Venn diagram showed that 2V shared fewer OTUs with other treatments (Figure S2b). Similar to microbial diversity, microbial structure in 2V was also significantly different from other treatments (Figure 3f; Table S1). Further analysis using LEfSe showed that distinct bacterial taxa were enriched under different carbon addition regimes (Figure 4). For ^{13}C-labeled microbial communities, Proteobacteria, Actinobacteria and Chloroflexi were significantly enriched in 2V, V and 1/2V treatment, respectively. Thees results confirmed that varying levels of carbon input invoke distinguishable microbial communities. Finally, correlation analysis revealed that both cumulative ^{13}C-CO_2 and CO_2 were significantly correlated with MBC and ^{13}C-DOC. Furthermore, cumulative ^{13}C-CO_2 was also significantly correlated with SOC and DOC (Figure 5).

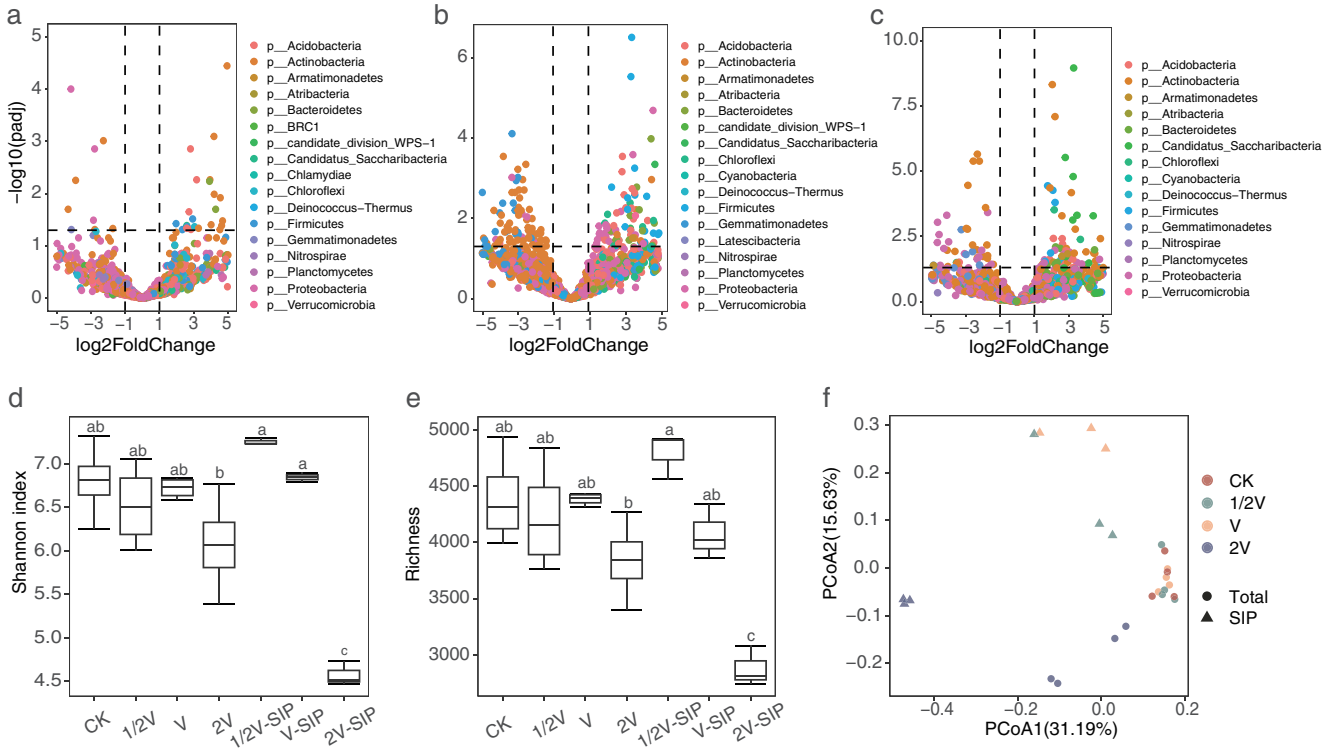


FIGURE 3 | Bacterial diversity and composition of the three glucose inputs rate (1/2V, V, and 2V root exudation rate of *Salix cupularis*) after 30 days' incubation. (a) Volcano plots showing the significant enriched bacterial taxa in 1/2V compared with CK. (b) Volcano plots showing the significant enriched bacterial taxa in V compared with CK. (c) Volcano plots showing the significant enriched bacterial taxa in 2V compared with CK. (d) Bacterial richness of each treatment. (e) Bacterial community Shannon index richness of each treatment. (f) Principal coordinate analysis of bacterial communities (Bray Curtis distance; Adonis, $p < 0.001$). Different letters indicate significant differences (one-way ANOVA, LSD test, $p < 0.05$). The central line represents the median and the error bars show standard error (SE). [Colour figure can be viewed at wileyonlinelibrary.com]

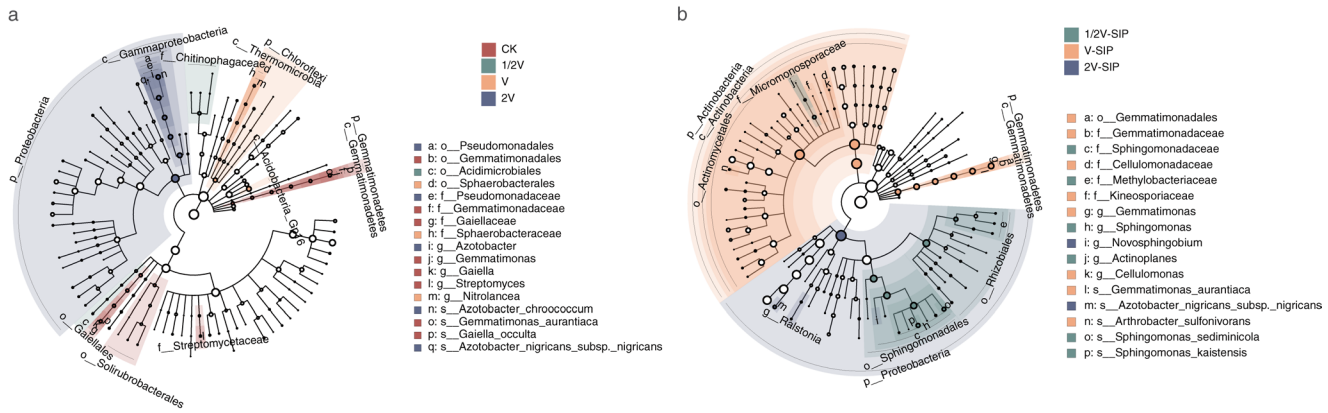


FIGURE 4 | LEfSe analysis showing the significantly enriched bacterial taxa in the three glucose input rates (1/2V, V, and 2V root exudation rate of *Salix cupularis*) after 30 days' incubation. (a) The whole bacterial community; (b) ^{13}C-labeled bacterial community. [Colour figure can be viewed at wileyonlinelibrary.com]

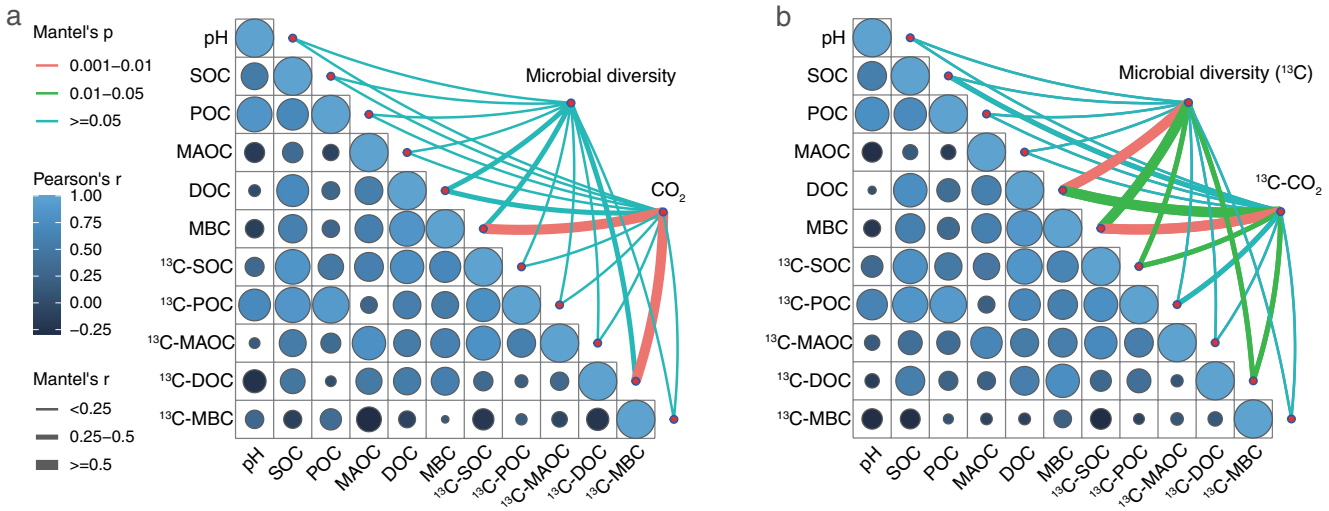


FIGURE 5 | Spearman correlation for soil properties and the Mantel test results showing the relationship between soil properties with bacterial diversity and cumulative CO_2 (a); ^{13}C-labeled bacterial diversity and cumulative ^{13}C-CO_2 (b). [Colour figure can be viewed at wileyonlinelibrary.com]

This pattern suggests that the primary pathway through which organic input affects the soil carbon pool in this sandy soil is by altering microbial activity.

4 | Discussion

4.1 | Responses of CO_2 Efflux and Carbon Sequestration to Glucose Addition Amount

Our results clearly demonstrate that the amount of simulated root exudates did not show linear impacts on CO_2 flux and C sequestration. We inferred that glucose input in V, approximates the natural root exudation rate of *S. cupularis*, is optimally suited to the microbial communities in this sandy soil. Lower C input (1/2V) can induce a priming effect that enhances the decomposition of native SOM, while higher inputs (2V) stimulate greater microbial respiration. Both scenarios ultimately result in a lower net efficiency of carbon sequestration into stable soil pools. This non-linear phenomenon is likely attributed to the adaptive metabolic strategies of microorganisms shaped by long-term environmental acclimatization (Robert et al. 2025). These findings consistently support our first hypothesis that ambient root carbon exudation minimizes soil CO2 efflux rates while promoting the accumulation and stabilization of SOC.

4.2 | Disproportionate Accumulation of POC Driven by C Inputs

The impact of varying glucose addition quantities on soil C components further highlights a non-linear trajectory, particularly concerning the priming effect and POC formation. While previous literature presents mixed conclusions on whether priming effects correlate positively or negatively with glucose quantity (Hu et al. 2025; Mo et al. 2022; Zhou et al. 2021), our study observed that lower C inputs (CK and 1/2V) led to lower POC, likely due to a combination of insufficient substrate and enhanced priming effects. Conversely, the significant accumulation of POC under V treatment suggests a threshold effect. In most cases, labile C inputs contribute predominantly to MAOC through microbial turnover, while physically fragmented plant residues are the primary source of POC (Yang et al. 2025). Since no labeled plant residues were added and no plants were cultivated in our microcosms, we suggested that the microbial community may play a primary role in transforming labile C to POC in V treatment. It is also supported by recent studies that up to 12.29% dissolved C input can be incorporated into POC through a microbe-mediated biochemical pathway (Si et al. 2024). We propose that microorganisms lean towards K-strategies; thus, limited C inputs are inadequate to shift their metabolic strategy, leading to lower POC use efficiency. While ambient inputs (V) provide the precise stoichiometric balance required to optimize microbial transformation of labile C into POC.

4.3 | Divergent Microbial Metabolic Strategies Dictate ^{13}C-Glucose Allocation

The metabolism of ^{13}C-glucose further confirmed that microbial carbon use efficiency and allocation do not follow a unified, linear trend with increasing C input. While MBC was highest in the 2V treatment, the accumulation of ^{13}C-MBC was lowest. This apparent paradox can be explained by divergent microbial life-history strategies triggered by varying substrate quantities. Microbial communities under lower C inputs (1/2V and V) likely prioritize storing labile carbon to survive nutrient-poor conditions. In contrast, the community under high C input (2V) rapidly metabolized and mineralized the available carbon to sustain high activity levels, resulting in a lower proportion of sequestered ^{13}C (Qiu et al. 2020). The relatively low overall transformation rate of ^{13}C-glucose to POC (about 5%) across treatments may be attributed to the inherently low initial soil C stock in sandy soils, compelling a large fraction of the added C to be allocated toward immediate microbial growth and respiration rather than stabilization (Wang et al. 2022). This aligns with previous studies showing that while microbes in C-limited soils rapidly assimilate soluble substrates, their actual substrate mineralization proportion remains distinctively decoupled from input quantity (He et al. 2025).

4.4 | High Carbon Inputs Reduce Microbial Diversity by Favoring Specialized Fermenters

Carbon inputs significantly modified soil microbial diversity and community structure, with the highest input (2V) invoking a severe drop in alpha diversity. Consistent with prior studies, we found that ^{13}C-labeled microbial community was compositionally distinct from the total community (Papp et al. 2020). The 2V treatment selectively enriched highly efficient, specialized sugar-fermenting microbes, such as specific taxa within Actinobacteria and the CPR group *Candidatus Saccharibacteria*, which thrive in sugar-rich environments by scavenging host-derived metabolites (He et al. 2024; Messyasz et al. 2024; Smith et al. 2022). This dominance competitively excluded other bacterial taxa, narrowing the ecological niche width and yielding a less stable microbial community structure (Brant et al. 2006; Feng et al. 2022). Interestingly, this resulted in an uncoupling of microbial diversity and activity, where 2V exhibited the highest soil respiration despite having the lowest diversity. Correlation analysis confirmed that organic input altered the soil C pool primarily by shifting microbial activity rather than diversity. While many studies emphasize microbial diversity in shaping soil C pools (Don et al. 2017; Xu et al. 2021), we argue that in severely degraded, resource-limited sandy soils, the immediate functional response of specialized existing microbes to a substantial carbon influx overrides overarching shifts in diversity as the dominant driver of short-term carbon dynamics.

While our study provides robust insights into the dosage-dependent mechanisms of SOC dynamics, simulating natural root exudation in vitro remains inherently complex. In this study, we utilized glucose as a model substrate to represent the labile carbon inputs of *S. cupularis*. Natural root exudates are highly complex mixtures comprising various sugars, organic acids, and amino acids. Future research should build upon this quantitative foundation by employing artificially synthesized ^{13}C-labeled compound mixtures to further untangle how exudate quality and quantity interactively drive the microbial carbon pump in desertified ecosystems.

5 | Conclusions

Our study reveals a non-linear relationship between the quantity of *S. cupularis* root exudates and SOC accrual. We found that varying levels of glucose input activate distinct microbial strategies: insufficient inputs induce a destructive priming effect that accelerates soil C loss, while excessive inputs reduce microbial diversity and carbon assimilation efficiency by favoring specialized fermenters. In contrast, ambient root exudation rates facilitate optimal plant-microbe interactions, promoting the microbe-mediated stabilization of labile carbon into POC. These findings emphasize that carbon input quantity is a pivotal driver of soil C pool dynamics. This knowledge not only deepens our understanding of plant-microbe adaptations in resource-limited environments but also offers actionable insights for optimizing organic amendments and selecting plant species for the ecological restoration of sandy soils.

Funding

This work was supported by the National Natural Science Foundation of China (32171616, 42577154, 32571899), Natural Science Foundation of Sichuan Province (2025ZNSFSC0202), Sichuan Forage Innovation Team Program (SCCXTD-2026-16). Science and Technology Department of Sichuan Province (2024NSFSC1965).

Conflicts of Interest

The authors declare no conflicts of interest.

Data Availability Statement

The data that support the findings of this study are available from the corresponding author upon reasonable request.

References

Ascenzi, I., J. P. Hilbers, M. M. van Katwijk, M. A. Huijbregts, and S. V. Hanssen. 2025. "Increased but Not Pristine Soil Organic Carbon Stocks in Restored Ecosystems." *Nature Communications* 16: 637.

Badri, D. V., and J. M. Vivanco. 2009. "Regulation and Function of Root Exudates." *Plant, Cell & Environment* 32: 666–681.

Biddle, J. F., S. Fitz-Gibbon, S. C. Schuster, J. E. Brenchley, and C. H. House. 2008. "Metagenomic Signatures of the Peru Margin Subseafloor Biosphere Show a Genetically Distinct Environment." *Proceedings of the National Academy of Sciences* 105: 10583–10588.

Brant, J. B., E. W. Sulzman, and D. D. Myrold. 2006. "Microbial Community Utilization of Added Carbon Substrates in Response to Long-Term Carbon Input Manipulation." *Soil Biology and Biochemistry* 38: 2219–2232.

Chari, N. R., and B. N. Taylor. 2022. "Soil Organic Matter Formation and Loss Are Mediated by Root Exudates in a Temperate Forest." *Nature Geoscience* 15: 1011–1016.

Ding, J., L. Chen, C. Ji, et al. 2017. "Decadal Soil Carbon Accumulation Across Tibetan Permafrost Regions." *Nature Geoscience* 10: 420–424.

Don, A., I. H. Böhme, A. B. Dohrmann, C. Poeplau, and C. C. Tebbe. 2017. "Microbial Community Composition Affects Soil Organic Carbon Turnover in Mineral Soils." *Biology and Fertility of Soils* 53: 445–456.

Edgar, R. C. 2016. "201cSINTAX: A Simple Non-Bayesian Taxonomy Classifier for 16S and ITS Sequences." *Biorxiv*: 074161.

Edgar, R. C., B. J. Haas, J. C. Clemente, C. Quince, and R. Knight. 2011. "UCHIME Improves Sensitivityand Speed of Chimera Detection." *Bioinformatics* 27: 2194–2200.

Feng, J., K. He, Q. Zhang, M. Han, and B. Zhu. 2022. "Changes in Plant Inputs Alter Soil Carbon and Microbial Communities in Forest Ecosystems." *Global Change Biology* 28: 3426–3440.

He, M., K. Fang, M. Tang, et al. 2025. "Weakened Priming Effect Along Soil Profile in Alpine Grasslands on the Tibetan Plateau." *Science China. Life Sciences* 68: 1–12.

He, W., H. Liang, W. Li, et al. 2024. "Revealing an Unprecedented Diversity of Episymbiotic Saccharibacteria in a High-Quality Genome Collection." *npj Biofilms and Microbiomes* 10: 153.

Hu, Y., J. Feng, S. Zhang, Z. Luo, and B. Zhu. 2025. "Adding Glucose at a Uniform Amount or According to Soil Organic Carbon Content Does Not Cause Significant Differences in Soil Priming Effects Across a Broad Grassland Transect." *Soil Ecology Letters* 7: 250333.

Hu, Y. F., X. Y. Shu, J. He, et al. 2018. "Storage of C, N, and P Affected by Afforestation With *Salix cupularis* in an Alpine Semiarid Desert Ecosystem." *Land Degradation & Development* 29: 188–198.

Huang, J., X. Zhou, G. Wu, et al. 2023. "Global Climate Impacts of Land-Surface and Atmospheric Processes Over the Tibetan Plateau." *Reviews of Geophysics* 61: e2022RG000771.

Kuzyakov, Y., J. Friedel, and K. Stahr. 2000. "Review of Mechanisms and Quantification of Priming Effects." *Soil Biology & Biochemistry* 32: 1485–1498.

Lange, M., N. Eisenhauer, C. A. Sierra, et al. 2015. "Plant Diversity Increases Soil Microbial Activity and Soil Carbon Storage." *Nature Communications* 6: 6707.

Li, Q., X. Shen, Q. Huang, et al. 2021. "Resource Islands of *Salix cupularis* Facilitating Seedling Emergence of the Companion Herbs in the Restoration Process of Desertified Alpine Meadow, the Tibetan Plateau." *Journal of Environmental Management* 289: 112434.

Li, Q., F. Yan, D. Chen, et al. 2025. "Root Exudates of *Salix cupularis* Orchestrate the Accumulation of Soil Carbon and Nitrogen in the Rhizosphere During the Restoration of a Desertified Alpine Meadow." *Applied Soil Ecology* 209: 106041.

Li, Q., C. Zhang, Y. Shen, W. Jia, and J. Li. 2016. "Quantitative Assessment of the Relative Roles of Climate Change and Human Activities in Desertification Processes on the Qinghai-Tibet Plateau Based on Net Primary Productivity." *Catena* 147: 789–796.

Li, X., D. Long, B. R. Scanlon, et al. 2022. "Climate Change Threatens Terrestrial Water Storage Over the Tibetan Plateau." *Nature Climate Change* 12: 801–807.

Liang, Y., D. Cao, Z. Ma, et al. 2024. "Stoichiometry Regulates Rice Straw-Induced Priming Effect: The Microbial Life Strategies." *Soil Biology & Biochemistry* 196: 109514.

Liao, J., X. Yang, Y. Dou, et al. 2023. "Divergent Contribution of Particulate and Mineral-Associated Organic Matter to Soil Carbon in Grassland." *Journal of Environmental Management* 344: 118536.

Love, M., S. Anders, and W. Huber. 2014. "Differential Analysis of Count Data–the DESeq2 Package." *Genome Biology* 15: 10–1186.

Luo, Z., E. Wang, and O. J. Sun. 2016. "A Meta-Analysis of the Temporal Dynamics of Priming Soil Carbon Decomposition by Fresh Carbon Inputs Across Ecosystems." *Soil Biology and Biochemistry* 101: 96–103.

McMurdie, P. J., and S. Holmes. 2013. "Phyloseq: An R Package for Reproducible Interactive Analysis and Graphics of Microbiome Census Data." *PLoS One* 8: e61217.

Messyasz, A., M. K. Männistö, L. J. Kerkhof, and M. M. Häggblom. 2024. "Genome Analysis and Description of Tunturibacter Gen. Nov. Expands the Diversity of Terriglobia in Tundra Soils." *Environmental Microbiology* 26: e16640.

Mo, F., C. Ren, K. Yu, et al. 2022. "Global Pattern of Soil Priming Effect Intensity and Its Environmental Drivers." *Ecology* 103: e3790.

Oksanen, J., F. G. Blanchet, R. Kindt, et al. 2013. "Package 'Vegan'." In *Community Ecology Package, Version.2*, 1–295.

Papp, K., B. A. Hungate, and E. Schwartz. 2020. "Glucose Triggers Strong Taxon-Specific Responses in Microbial Growth and Activity: Insights From DNA and RNA qSIP." *Ecology* 101: e02887.

Qiu, G., M. Zhu, M. Contin, et al. 2020. "Evaluating the 'Triggering Response' in Soils, Using 13C-Glucose, and Effects on Dynamics of Microbial Biomass." *Soil Biology & Biochemistry* 147: 107843.

Robert, C. A. M., P. Himmighofen, S. McLaughlin, et al. 2025. "Environmental and Biological Drivers of Root Exudation." *Annual Review of Plant Biology* 76: 317–339.

Segata, N., J. Izard, L. Waldron, et al. 2011. "Metagenomic Biomarker Discovery and Explanation." *Genome Biology* 12: R60.

Si, Q., K. Chen, B. Wei, Y. Zhang, X. Sun, and J. Liang. 2024. "Dissolved Carbon Flow to Particulate Organic Carbon Enhances Soil Carbon Sequestration." *Soil* 10: 441–450.

Smith, D. J., J. J. Kharbush, R. D. Kersten, and G. J. Dick. 2022. "Uptake of Phytoplankton-Derived Carbon and Cobalamins by Novel Acidobacteria Genera in Microcystis Blooms Inferred From Metagenomic and Metatranscriptomic Evidence." *Applied and Environmental Microbiology* 88: e01803-21.

Tao, F., Y. Huang, B. A. Hungate, et al. 2023. "Microbial Carbon Use Efficiency Promotes Global Soil Carbon Storage." *Nature* 618: 981–985.

Wang, G., M. Wang, X. Guo, Y. Yu, P. Han, and Z. Luo. 2022. "Efficiency of Additional Organic Inputs for Carbon Sequestration in Agricultural Soils Modulated by the Priming Effect and Physical Accessibility." *Geoderma* 406: 115498.

Wang, Q., L. Chen, Q. Yang, et al. 2019. "Different Effects of Single Versus Repeated Additions of Glucose on the Soil Organic Carbon Turnover in a Temperate Forest Receiving Long-Term N Addition." *Geoderma* 2019, no. 341: 59–67.

Xia, W., C. Zhang, X. Zeng, et al. 2011. "Autotrophic Growth of Nitrifying Community in an Agricultural Soil." *ISME Journal* 5: 1226–1236.

Xu, M., X. Li, T. W. Kuyper, M. Xu, X. Li, and J. Zhang. 2021. "High Microbial Diversity Stabilizes the Responses of Soil Organic Carbon Decomposition to Warming in the Subsoil on the Tibetan Plateau." *Global Change Biology* 27: 2061–2075.

Yan, F., Q. Huang, D. Chen, et al. 2025. "Palmitic Acid Triggers Rhizosphere Acidification to Facilitate Microbial Nitrogen Fixation: A Perspective for Phytoremediation of Desertification Alpine Grassland via Artificial Root Exudation Mimicking." *Journal of Environmental Management* 390: 126349.

Yang, Y., A. Gunina, H. Cheng, et al. 2025. "Unlocking Mechanisms for Soil Organic Matter Accumulation: Carbon Use Efficiency and Microbial Necromass as the Keys." *Global Change Biology* 31: e70033.

Yilmaz, P., L. W. Parfrey, P. Yarza, et al. 2014. "The SILVA and "All-Species Living Tree Project (LTP)" Taxonomic Frameworks." *Nucleic Acids Research* 42, no. D1: D643–D648.

Yu, M., Y.-P. Wang, Q. Deng, et al. 2024. "Soil Acidification Enhanced Soil Carbon Sequestration Through Increased Mineral Protection." *Plant and Soil* 503: 529–544.

Yuan, Y., W. Zhao, Z. Zhang, et al. 2018. "Impacts of Oxalic Acid and Glucose Additions on N Transformation in Microcosms via Artificial Roots." *Soil Biology and Biochemistry* 121: 16–23.

Zhang, J., and M. J. Zhang. 2013. "Package 'spaa'." R Package Version, 1, 10–32614.

Zhou, J., Y. Wen, L. Shi, et al. 2021. "Strong Priming of Soil Organic Matter Induced by Frequent Input of Labile Carbon." *Soil Biology and Biochemistry* 152: 108069.

Supporting Information

Additional supporting information can be found online in the Supporting Information section. **Table S1:** PERMANOVA test (999 permutations) of bacterial structures in the three glucose inputs rate (1/2 V, V, and 2 V root exudation rate of *Salix cupularis*) after 30 days' incubation. **Figure S1:** Study site (a) and microcosm used for incubation experiment (b). **Figure S2:** Bacterial community compositions in the three glucose inputs rate (1/2 V, V, and 2 V root exudation rate of *Salix cupularis*) after 30 days' incubation. (a) Top 10 bacterial phylum of each treatment. (b) Venn diagram showing the shared OUT among treatments. **Figure S3:** Priming effect of the three glucose inputs rate (1/2 V, V, and 2 V root exudation rate of *Salix cupularis*) after 30 days' incubation. **Figure S4:** Bacterial niche width of the three glucose inputs rate (1/2 V, V, and 2 V root exudation rate of *Salix cupularis*) after 30 days' incubation. The central line represents the median and the error bars showed standard error (SE).